Global and Stochastic Analysis
Vol. 12 No. 2 (March, 2025)

Received: 18th December 2024 *Revised: 06th January 2025* *Accepted: 25th January 2025*

WILLIAMSON NANOFLUID FLOW OF THERMALLY RADIANT PERMEABLE STRETCHING SHEET WITH JOULE HEATING EFFECTS AND CHEMICAL REACTION

KEMPARAJU M.C, B.LAVANYA, RAVEENDRA NAGARAJ,
MAHANTESH M. NANDEPPANAVAR, AND NAGARATHNA T. K.

Abstract. This study investigates the behavior of incompressible flow over a permeable stretched sheet, considering the effects of viscous dissipation and Joule heating in a constant two-dimensional electrically conducting, thermally radiant Williamson Nanofluid. Employing suitable transformation equations reduces the governing partial differential equations to a set of nonlinear ordinary differential equations. These equations are subsequently solved numerically using the standard fourth-order Runge-Kutta method in conjunction with the shooting technique. The results are presented graphically, illustrating the flow, temperature, and nanoparticle volume fraction profiles. The research examines how various physical characteristics influence heat and mass transfer rates, including temperature, velocity, skin friction coefficient, and nanoparticle volume percentage.

1. Introduction

Williamson nanofluid refers to a type of nanofluid that behaves according to Williamson fluid model, which describes non-Newtonian fluid behavior. Non-Newtonian fluids possess viscosities that vary with shear stress or strain rate, in contrast to Newtonian fluids (such as water or air), which maintain a constant viscosity. The Williamson model describes fluids that demonstrate shear-thinning behavior, indicating that their viscosity decreases as the shear rate increases. This is often encountered in polymers, biological fluids, and certain industrial fluids. Nanofluids are fluids containing nanoscale particles (nanoparticles), which can enhance thermal conductivity, electrical conductivity, or other properties of the base fluid. These particles can be metals, oxides, or carbon-based materials. A Williamson nanofluid combines the shear-thinning characteristics of the Williamson model with enhanced thermal properties of nanofluids. These fluids are often used in engineering and heat transfer applications, such as cooling systems, thermal management, and energy storage. Viscous dissipation refers to the process by which mechanical energy is converted into heat due to the action of viscosity in a fluid. It occurs when a fluid flows and experiences internal friction between its layers, which leads to the transformation of kinetic energy into thermal energy. This phenomenon is important in many areas of fluid dynamics and

2000 *Mathematics Subject Classification.* 34B15; 76D05.
Key words and phrases. Williamson Nanofluid, Stretching Sheet,Viscous Dissipation, Electrically Conducting Fluid, Thermal Radiation, Velocity Slip Boundary Condition.

heat transfer, particularly in high-viscosity fluids or under extreme shear conditions. Choi[1] described enhancing thermal conductivity of fluids with nanoparticles. Sbragaglia and Prosperetti[2] studied nature of effective velocity boundary condition for liquid flow over a plane boundary on which small free-slip islands are randomly distributed. The problem of laminar fluid flow resulting from the stretching of a flat surface in a nanofluid has been investigated numerically first time by Khan and Pop[3]. In the presence of nanoparticle fractions and on considering the dynamic effects including the Brownian motion and thermophoresis, the developments of the second order slip velocity on the boundary layer flow and heat transfer over a stretching surface is presented by Emad[4]. Radiation and chemical reaction effects on the steady boundary layer flow of MHD Williamson fluid through porous medium toward a horizontal linearly stretching sheet in the presence of nanoparticles are investigated numerically by Krishnamurthy et al.[5]. The "blade coating analysis of a Williamson fluid" likely involves studying the behavior of a non-Newtonian fluid (specifically a Williamson fluid) during the blade coating process, which is commonly used in industrial applications like printing, coating, and film manufacturing explained by Siddique et al.[6].Krishna and Chamkha [7]involved in a detailed analysis of heat and mass transfer in a magnetohydrodynamic (MHD) flow of a second-grade fluid through a porous medium over a semi-infinite vertical stretching sheet. Tesfaye Kebede et al.[8] investigated the analytic approximation to the heat and mass transfer characteristics of a two-dimensional time-dependent flow of Williamson nanofluids over a permeable stretching sheet embedded in a porous medium has been presented by considering the effects of magnetic field, thermal radiation, and chemical reaction. The MHD boundary layer flow of a nanofluid past a stretching/shrinking sheet with hydrodynamic, thermal, and solutal slip boundary conditions was studied by Mansur and Ishak [9]. Ali et al. [10] elaborated the natural convection of a magnetohydrodynamic nanofluid in an enclosure under the effects of thermal radiation and the shape factor of nanoparticles was analyzed numerically using the control-volume-based finite element method. Magnetic nanofluid natural convection in the porous enclosure considering Brownian motion is studied numerically using CVFEM by Dogonchi et al.[11]. Sejunti and Khaleque [12]reported the flow and heat transfer of ferrofluids over a flat plate with slip conditions and radiation using the Keller-Box method. Hall and ion slip effects on magnetohydrodynamic free convective rotating flow of nanofluids in a porous medium past a moving vertical semi-infinite flat plate are investigated by Veer Krishna and Chakha [13]. The slip boundary condition for nanoflows is crucial aspect of nanohydrodynamics theory and significantly influences design and fabrication of nanofluidic devices. Ruifei Wang et al.[14] In this review, focused on the slip boundary conditions for nanoconfined liquid flows.velocity slip boundary condition has significant implications for the flow and heat transfer characteristics of non-Newtonian ferrofluids over a stretching sheet. It alters the momentum transfer, modifies the shear stress, and influences the behavior of magnetic particles within the fluid examined by Hussan Zeb et al.[15]. The combined effect of hybrid nanoparticle and velocity slip Boundary Conditions on the nonlinear problem of MHD Jeffery–Hamel flow described by Mohamed Kezzar et al.[16]. Dawood et al.[17] analyzed the pulsatile nano-blood

flow through a sinusoidal wavy channel, emphasizing the significance of diverse influences in the modelling. Hui WU et al.[18] concentrated on the rarefaction effect coupled with the roughness effect on surface properties to replace the slip boundary condition at the smooth surface with an effective boundary condition modified by roughness. Azad Hussain [19] presented report on Transportation of thermal and velocity slip factors on three-dimensional dual phase nanomaterials liquid flow towards an exponentially stretchable surface. Mathematical study of Slip conditions on electrically conducting nanofluid over a vertically stretching sheet is presented with effects of viscous dissipation, thermal radiation and Soret and Dufor by Al- Zubaidi et al. [20]. Lavanya et al. [21] the study of multiple slip effects on the time independent MHD flow of a UCM fluid over an elongating surface with chemical reaction. Non-Newtonian nanofluid under magnetohydrodynamics (MHD) and radiation effects through slender cylinder elaborated by Saquib Ul Zaman et al. [22]. Siva Shanakari et al.[23] investigated on the drift of an MHD Williamson liquid past an extended sheet under the influence of Joule heating. Vinod Kumar Reddy et al.[24] explored the effect of activation energy on the MHD radiative Williamson nanofluid flow across a wedge using heat generation and binary chemical reactivity. In The present paper we investigate the behavior of incompressible flow over a permeable stretched sheet, considering the effects of viscous dissipation and Joule heating in a constant two-dimensional electrically conducting, thermally radiant Williamson Nanofluid. Employing suitable transformation equations reduces the governing partial differential equations to a set of nonlinear ordinary differential equations. These equations are subsequently solved numerically using the standard fourth-order Runge-Kutta method in conjunction with the shooting technique. The results are presented graphically, illustrating the flow, temperature, and nanoparticle volume fraction profiles. The research examines how various physical characteristics influence heat and mass transfer rates, including temperature, velocity, skin friction coefficient, and nanoparticle volume percentage. Findings indicates that velocity ratio parameter decreases the mass transfer rate while increasing the skin friction coefficient, velocity profile, and heat transfer rate. In contrast, increasing mass injection enhances both temperature profiles and velocity. In contrast, a rise in mass suction parameter reduces temperature and velocity boundary layer thickness, albeit significantly accelerating heat transfer. Additionally, while non-Newtonian parameter decreases nanofluid's mass transfer rate and velocity, it increases heat transfer rate.

2. FORMULATION OF THE PROBLEM

Consider uniform free stream of an incompressible Williamson nanofluid that conducts electricity and is thermally radiant, flowing steadily in two dimensions over a permeable stretched sheet; joule heating effects and viscous dissipation are also discussed. Assume that plate is extending at a velocity of $u_w = ax(a > 0)$, where a is stretching parameter, and that velocity of free stream is $u_\infty = bx(b > 0)$. The plate is subjected to a constant external magnetic field B_0. It is less probable for electrons to collide with other charged or neutral particles in succession due to presence of a nanofluid (as opposed to an ionized gas) when an external magnetic field is applied. This reduced electron-atom collision frequency

allows us to ignore electric field from charge polarization and effects of ion slip and Hall. The temperature and nanoparticle concentration at moving surface are assumed to be constant values, denoted as (T_w) and (C_w), respectively. Under these assumptions, governing boundary-layer equations for momentum, energy, and diffusion of thermally radiating Williamson nanofluid in presence of a free stream can be expressed as follows:

$$\frac{\partial u}{\partial x}+\frac{\partial v}{\partial y}=0 \tag{1}$$

$$u\frac{\partial u}{\partial x}+v\frac{\partial v}{\partial y}=v\frac{\partial^2 u}{\partial y^2}+\sqrt{2}v\Gamma\frac{\partial u}{\partial y}\frac{\partial^2 u}{\partial y^2}+u_\infty\frac{\partial u_\infty}{\partial x}+\frac{\sigma B_0^2}{\rho}(u_\infty-u) \tag{2}$$

$$u\frac{\partial T}{\partial x}+v\frac{\partial T}{\partial y}=\alpha\frac{\partial^2 T}{\partial y^2}+\frac{v}{c_p}\left[\left(\frac{\partial u}{\partial y}\right)^2+\sqrt{2}\Gamma\left(\frac{\partial u}{\partial y}\right)^3\right]+\tau\left[D_B\frac{\partial C}{\partial y}\frac{\partial T}{\partial y}+\frac{D_T}{T_\infty}\left(\frac{\partial T}{\partial y}\right)^2\right]$$
$$+\frac{\sigma B_0^2}{\rho C_p}(u-u_\infty)^2-\frac{1}{\rho c_p}\frac{\partial q_r}{\partial y} \tag{3}$$

$$u\frac{\partial C}{\partial x}+v\frac{\partial C}{\partial y}=D_B\frac{\partial^2 C}{\partial y^2}+\frac{D_T}{T_\infty}\frac{\partial^2 T}{\partial y^2}-K_r(C-C_\infty) \tag{4}$$

where, in x and y directions, respectively, u and v are the velocity components; T is for temperature, while C is volume percentage of nanoparticles. The values of σ,α and C_p correspond to nanofluid's electrical conductivity, thermal diffusivity, and specific heat capacity, respectively; D_B, D_T, K_r and Γ stand for Brownian diffusion coefficient, thermophoresis diffusion coefficient, chemical reaction constant and time constant; ρ, μ and k are the density, kinematic viscosity, and thermal conductivity of the nanofluid; q_r is radiative heat flux, Γ is ratio of fluid's heat capacity to that of nanoparticles.

The boundary conditions associated with differential equations are:

$$\begin{aligned} &u=U_w+u_{\text{slip}}, \quad v=-V_w, \quad T=T_w, \quad C=C_w \quad \text{at } y=0,\\ &u\to\infty, \quad T\to T_\infty, \quad C\to C_\infty \quad \text{as } y\to\infty. \end{aligned} \tag{5}$$

where T_∞ and C_∞ stand for temperature and the volume percentage of far-from-the-sheet nanoparticles, respectively. The mass suction/injection velocity is denoted by the word V_w. For suction, it expresses the mass to be transported at the surface with $V_w>0$, and for injection, it uses $V_w<0$. The radiative heat flux q_r is determined by using the Rosseland diffusion approximation.

$$q_r=\frac{-4\sigma^*}{3K^*}\frac{\partial T^4}{\partial y} \tag{6}$$

where σ^* is Stefan-Boltzmann constant and k^* is mean absorption coefficient. T^4 can be expressed as a linear function of T since it is expected that temperature variations within flow are quite small: The following system of equations are set to reduce governing equations into a system of odes:

$$\eta=y\sqrt{\frac{a}{v}}, T=T_\infty+(T_w-T_\infty)\theta(\eta) \tag{7}$$

$$C=C_\infty+(C_w-C_\infty)\phi(\eta), \quad \psi=\sqrt{av}\,f(\eta) \tag{8}$$

Where,

$$f''' + ff'' + Wef''f''' - f'^2 + M(A - f'^2) + A^2 = 0 \tag{9}$$

$$\left(1 + \frac{4}{3}Rd\right)\theta'' + Pr\left(f\theta' + Ecf''^2\right) + Wef''' + Mf'^2 + Nb\theta'\phi' + Nt\theta'^2 = 0 \tag{10}$$

$$\phi' + Scf\phi' + \frac{Nt}{Nb}\theta'' - ScK_1\phi = 0 \tag{11}$$

And associated boundary conditions becomes:

$$f(0) = S, f'(0) = 1 + \lambda f''(0), \theta(0) = 1, \phi(0) = 1 \tag{12}$$

$$f'(\eta) \to A, \quad \theta'(\eta) \to 0, \quad \phi(\eta) \to 0 \quad \text{as} \quad \eta \to \infty \tag{13}$$

$$c_f = \frac{\tau_w}{\rho U_w^2}, Nu_x = \frac{xq_w}{k(T_w - T_\infty)}, Sh_x = \frac{x/w}{D_B(C_w - C_\infty)} \tag{14}$$

$$\tau_w = \mu\left[\frac{\partial u}{\partial y} + \frac{\Gamma}{\sqrt{2}}\left(\frac{\partial u}{\partial y}\right)^2\right]_{y=0} \tag{15}$$

$$q_w = -\left(K + \frac{16\sigma^* T_\infty^3}{3K^*}\right)\left(\frac{\partial C}{\partial y}\right)_{y=0}, \quad J_w = -D_B\left(\frac{\partial C}{\partial y}\right)_{y=0} \tag{16}$$

3. Numerical Solution

The shooting method is numerical technique to solve boundary value problems (BVPs) for ordinary differential equations (ODEs). In boundary value problems (BVPs), boundary conditions are specified at edges of domain. This differs from initial value problems, which typically depend on initial conditions. Given that equations (10) to (12) are highly nonlinear, finding closed-form solutions can be challenging, if not impossible. Consequently, these boundary value problems are solved numerically using conventional fourth-order Runge-Kutta integration method in conjunction with shooting technique. The core concept of shooting method involves transforming boundary value problem into an initial value problem. To achieve this, one must make an educated guess regarding unknown initial conditions at one of boundaries. This guessed initial condition is then used to solve the ODE as if it were an initial value problem, utilizing standard numerical methods such as Runge-Kutta or Euler's method. The resulting solution spans entire domain, allowing for comparison of value at other boundary with the actual boundary condition stipulated in problem. If the computed solution does not satisfy required boundary condition, it indicates that initial guess was incorrect. In this case, initial guess must be modified, and initial value problem must be solved again. Various techniques can be employed to adjust the initial guess, including root-finding methods like Newton's method, which iteratively refines guess until boundary condition at the far end is satisfied. This process is repeated until solution meets boundary conditions at both ends within specified tolerance.

Let $f_1 = F$, $f_2 = F_1'$, $f_3 = F_2'$, $f_4 = \theta$, $f_5 = \theta'$, $f_6 = \phi$, $f_7 = \phi'$ then

$$F''' = -\frac{F_1F_3 + F_2^2 - M(A - F_2) - A^2}{1 + WeF_3} \tag{1}$$

$$\theta'' = -\frac{Pr}{1 + (4/3)Rd}(F_1F_5 + Ec((F_3)^2) + We(F_3)^3) + M(F_2)^2 + NbF_5F_7 + Nt(F_5)^2 \tag{2}$$

$$\phi'' = -ScF_1F_7 + K_1ScF_6 + \frac{NtPr}{Nb(1 + (4/3)Rd)}$$
$$(F_1F_5 + Ec((F_3)^2 + We(F_3)^3 + M(F_2)^2) + NbF_5F_7 + Nt(F_5)^2 \tag{3}$$

With the boundary conditions

$$F_1(0) = S, F_2(0) = 1, F_4(0) = 1, F_6(0) = 6, F_2(\infty) = A, F_4(\infty) = 0, F_6(\infty) = 0) \tag{4}$$

To integrate (17)-(19) as an initial value problem, no need to find values of

$$F_3(0) = p, \quad F_5(0) = q, \quad \text{and} \quad F_7(0) = r$$

The values are not defined within the boundary conditions described in equation (20). The primary objective of the shooting method is to identify suitable finite values. To solve the boundary value problem outlined in equations (17) to (20), we begin by making initial guesses based on a specific set of physical parameters. This will enable us to determine $f''(0)$, $\theta'(0)$, and $\phi'(0)$, which differ by pre-assigned significant digits.

The last value of η_∞ is finally chosen to be the most appropriate value of η_∞ for that set of parameters. The value of η_∞ may vary for another set of parameters. Once the finite value of η_∞ is determined, integration is carried out easily.

Accordingly, the initial condition vector for the boundary value problem is given by:

$$Y_0 = [S, 1, p, 1, q, 1, r].$$

We took a series of values for $f''(0)$, $\theta'(0)$, and $\phi'(0)$, and applied a fourth-order Runge-Kutta (RK) integration scheme with a step size $h = 0.001$. The above procedure was repeatedly performed until the desired degree of accuracy 10^{-6} was obtained.

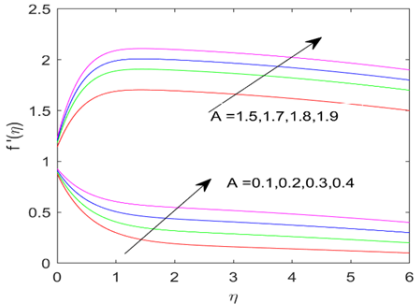

FIGURE 1. Velocity profiles for values of A

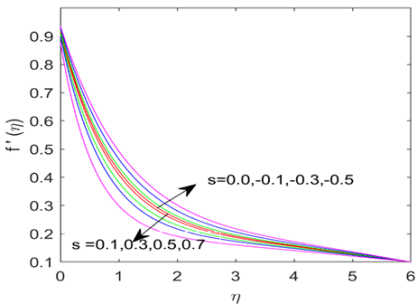

FIGURE 2. Velocity profiles for values of S

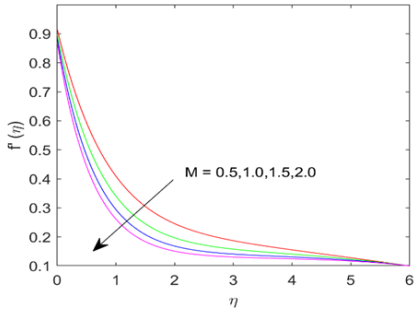

FIGURE 3. Velocity profiles for values of M

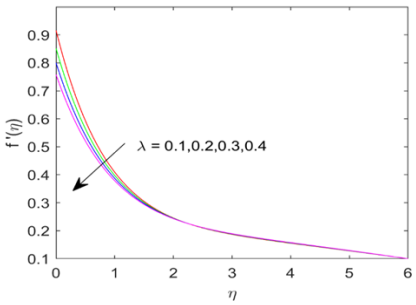

FIGURE 4. Velocity profiles for values of λ

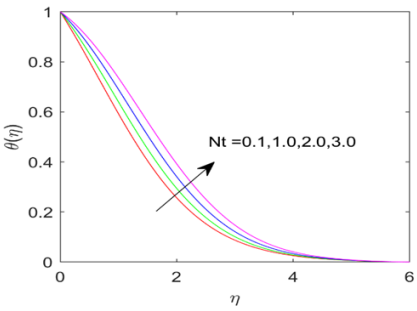

FIGURE 5. Temperature profiles for values of Nt

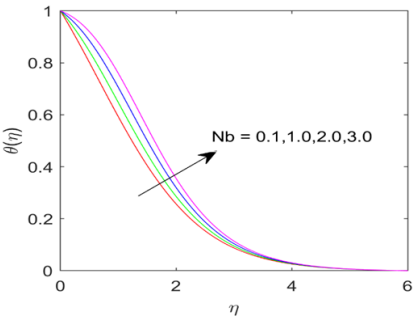

FIGURE 6. Temperature profiles for values of Nb

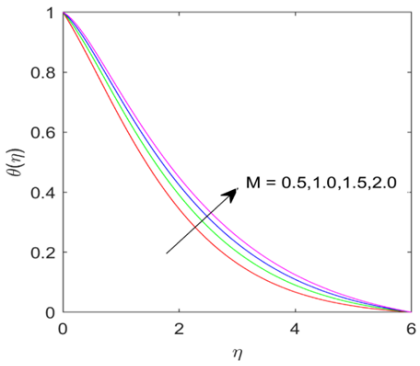

FIGURE 7. Temperature profiles for values of M

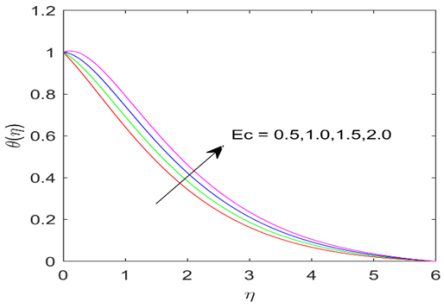

FIGURE 8. Temperature profiles for values of Ec

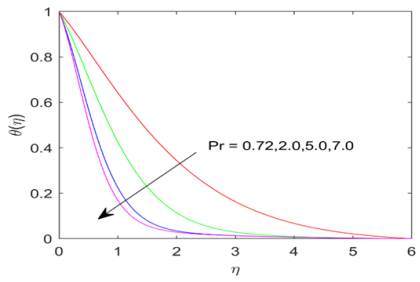

FIGURE 9. Temperature profiles for values of Pr

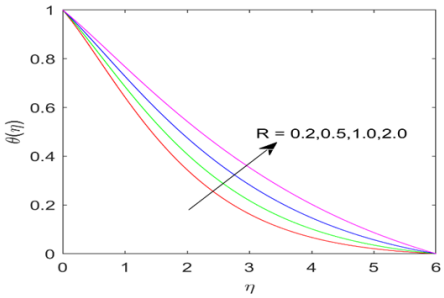

FIGURE 10. Temperature profiles for values of R

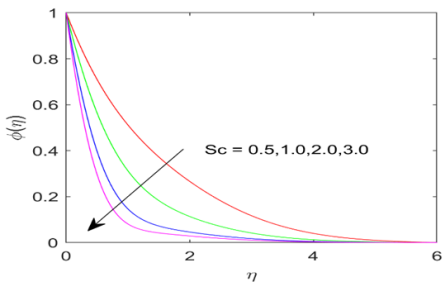

FIGURE 11. Concentration profiles for values of Sc

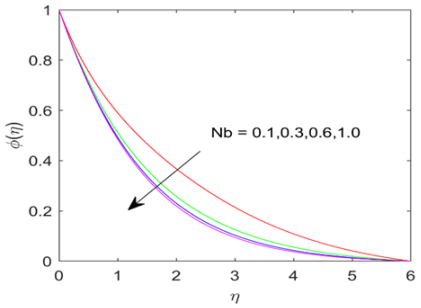

FIGURE 12. Concentration profiles for values of Nb

The deviations of $f'(\eta)$ has been noticed in Fig. 1. The effect of velocity ratio parameter on velocity distributions is an important topic in fluid dynamics, particularly in the study of boundary layers, jets, and wakes. The velocity ratio parameter is typically defined as the ratio of velocity of one fluid stream to another, and it plays a critical role in determining the behavior of velocity distributions. In boundary layer flows, the velocity ratio between free stream and the wall can influence the thickness and shape of the boundary layer. A higher velocity ratio generally leads to a thinner boundary layer, while a lower velocity ratio results in a thicker boundary layer. This parameter also affects the velocity gradient near the wall, which has implications for shear stress and heat transfer rates. In jet flows, the velocity ratio between the jet and the surrounding fluid influences spreading rate of the jet. A higher velocity ratio typically results in a narrower, faster jet with less entrainment of the surrounding fluid. Conversely, a lower velocity ratio leads to a wider jet with more mixing and entrainment. The velocity distribution within the jet itself also depends on the velocity ratio, with higher ratios leading to more uniform velocity profiles along the jet axis. In wake flows, such as those behind bluff bodies, the velocity ratio between the wake and the free stream affects the wake width and the velocity deficit. A higher velocity ratio generally results in a narrower wake with a smaller velocity deficit, while a lower ratio leads to a wider wake and a larger velocity deficit. The velocity distribution in the wake region is also influenced by the velocity ratio, with significant impacts on the drag and lift forces experienced by the object generating the wake. The velocity ratio can significantly impact the mixing efficiency and stability of flow configurations, such as in shear layers or between two fluid streams of different velocities. A high velocity ratio can lead to increased shear and potential instabilities, while a lower ratio might result in more stable, yet less mixed flows.

The wall transfer parameter, often referred to context of heat or mass transfer at the boundary of a fluid system (such as a wall), plays a significant role in the velocity profile of fluid flow, particularly in boundary layer theory or near-wall phenomena in fluid dynamics. Fig. 2 explains the impression of wall transfer

parameter on velocity distributions. Increased wall transfer (heat or mass) can alter the boundary layer thickness and modify the velocity gradient near the wall. Decreased wall transfer may produce a velocity profile that is closer to the ideal, where momentum is the primary driving force, without additional thermal or concentration effects. The impact of magnetic parameter on velocity distributions is significant and varies depending on the flow configuration and the strength of the magnetic field has been observed in Fig.3. Lorentz Force: The magnetic field interacts with moving charged particles in the fluid, generating a Lorentz force that opposes the motion. This force acts as a form of drag on fluid, which leads to a reduction in velocity of the flow. As magnetic parameter increases, this damping effect becomes more pronounced, resulting in lower overall fluid velocities. Velocity Profile Flattening: In many MHD flows, an increase in magnetic parameter flattens velocity profile. This means that difference in velocity between the fluid at the boundary and the fluid in the core decreases, leading to a more uniform flow distribution across the cross-section of the flow. Thickening of the Boundary Layer: The presence of magnetic field can lead to an increase in boundary layer thickness. This is because Lorentz force dampens flow near wall, which reduces velocity gradient at boundary and causes the boundary layer to thicken. This effect is particularly notable in Hartmann flows, where the fluid is driven through a channel under influence of a strong magnetic field. Fig.4 describes impact of slip parameter on $f'(\eta)$. The velocity slip parameter plays a significant role in controlling the behavior of fluid flow near surfaces, particularly when there is a difference between the velocity of the fluid at the boundary (or surface) and velocity of the boundary itself. In classical fluid mechanics, no-slip boundary conditions are typically assumed, meaning fluid velocity at a solid boundary is zero relative to the boundary. However, in certain cases (such as microflows, rarefied gas flows, or specific porous media flows), no-slip condition is no longer valid, and velocity slip must be considered. The velocity slip parameter λ determines degree of slip at boundary, which in turn affects velocity distribution of the fluid. Here's how velocity slip parameter influences velocity distribution: No Slip: Velocity at the boundary is zero, and velocity distribution grows from zero at the wall, resulting in a steep velocity gradient. Partial Slip: With increasing slip parameter λ , fluid velocity near the wall is non-zero, leading to a flatter velocity profile near the boundary and a higher overall fluid velocity. High Slip: At high slip values, velocity profile becomes nearly uniform, with the boundary contributing little resistance, and shear stress near the wall decreases. Thermophoresis refers to movement of particles in a fluid due to a temperature gradient. The consequences of thermophoresis parameter on $\theta(\eta)$ is showed in Fig. 5. When considering the effect of the thermophoresis parameter on temperature distributions in a fluid,$\theta(\eta)$ increases and particularly in contexts like heat transfer and fluid dynamics, several key points can be observed: Temperature Gradient Influence: The thermophoresis parameter is proportional to the temperature gradient within the fluid. A higher temperature gradient enhances the thermophoretic force, which can cause particles to move more quickly from regions of high temperature to regions of lower temperature. Heat Transfer Enhancement: In systems where thermophoresis is significant, particles that move towards cooler regions can affect local temperature distribution. This movement

can either enhance or reduce overall heat transfer depending on system's specific conditions, such as nature of fluid and boundary conditions. Boundary Layer Effects: In boundary layer flows, thermophoresis can alter temperature distribution near wall. If particles are drawn towards a cooler boundary, they can create a layer of particles that insulates or increases thermal resistance, potentially affecting the temperature profile near the surface. Non-Uniform Temperature Profiles: The presence of thermophoresis can lead to non-uniform temperature profiles within the fluid. For instance, in systems with a strong temperature gradient, particles may cluster in certain regions, leading to localized changes in temperature distribution. Impact on Cooling/Heating Efficiency: In applications such as cooling technologies, where particles are introduced into a fluid for heat removal, the thermophoresis effect can influence how effectively heat is transferred. By controlling the thermophoresis parameter, engineers can optimize cooling or heating process. Analytical and Numerical Modeling: In many studies, effect of the thermophoresis parameter on temperature distributions is analyzed through analytical models or numerical simulations. These models help predict how varying the parameter impacts the overall temperature field within the fluid. Brownian motion refers to random motion of particles suspended in a fluid, resulting from collisions with molecules of fluid. The changes in $\theta(\eta)$ has shown in Fig. 6. In the context of heat transfer and fluid dynamics, the Brownian motion parameter plays a significant role in influencing temperature profile of the fluid-particle system. Diffusion of Particles: The Brownian motion parameter is directly related to intensity of the random movement of particles. Higher Brownian motion results in more vigorous diffusion of particles throughout the fluid. This enhanced mixing can lead to a more uniform temperature distribution, as the particles disperse heat more effectively. Thermal Conductivity Enhancement: In nanofluids (fluids containing nanoparticles), the Brownian motion of nanoparticles contributes to an increase in effective thermal conductivity. As particles move randomly, they carry energy across the fluid, which can smooth out temperature gradients and alter the temperature profile. Temperature Profile Smoothing: Due to the enhanced mixing and energy transfer caused by Brownian motion, the temperature profile in the fluid tends to become smoother. Sharp temperature gradients are reduced, and the temperature distribution becomes more homogeneous. Boundary Layer Effects: In boundary layer flows, Brownian motion can affect the temperature distribution near the solid surface. The random movement of particles can disrupt the thermal boundary layer, leading to a change in the temperature gradient close to the wall. This effect can either increase or decrease the heat transfer rate, depending on the system's specifics. Impact on Nanofluid Heat Transfer: In nanofluids, Brownian motion of nanoparticles is a key factor in enhancing heat transfer. By increasing the Brownian motion parameter, thermal conductivity of fluid improves, which can lead to a more efficient heat transfer process. Consequently, temperature profile may show a more rapid decrease in temperature with distance from heat source. On-Uniform Temperature Distribution: In some cases, particularly at low Brownian motion, particles may not disperse evenly, leading to non-uniform temperature distributions. This can result in localized hot or cold spots within fluid, impacting the overall heat transfer efficiency. Fig. 7 addresses the influence of magnetic

parameter on temperature profile. When studying the impact of the magnetic parameter on the temperature profile in such a system, several key effects can be observed. The magnetic parameter plays a significant role in modifying the temperature profile of a conducting fluid by influencing fluid motion, altering heat transfer rates, and affecting the thermal boundary layer. A stronger magnetic field typically leads to a more stratified temperature distribution with steeper gradients, particularly in the vicinity of heated or cooled surfaces. The influence of the Eckert number on temperature distributions can be understood through the following points through the Fig. 8. Viscous Dissipation: The Eckert number quantifies the contribution of viscous dissipation to the overall heat transfer. In flows with a high Eckert number, the viscous dissipation is significant, leading to the generation of heat within the fluid. This additional heat alters the temperature distribution, typically increasing the temperature in the flow field. Temperature Rise in Boundary Layers: In boundary layers, where viscous effects are more pronounced, a high Eckert number can lead to a substantial temperature rise near the wall. This is because the kinetic energy of the fluid is converted into thermal energy through viscous dissipation, which heats up the fluid near the boundary. Impact on Thermal Boundary Layer: The presence of a high Eckert number can thicken the thermal boundary layer due to the additional heat generated by viscous dissipation. This results in a steeper temperature gradient near the wall and affects the overall temperature distribution within the boundary layer. Temperature Distribution in Compressible Flows: In compressible flows, especially at high velocities (such as in supersonic or hypersonic flows), the Eckert number becomes more significant. The kinetic energy of the flow is substantial, and viscous dissipation can lead to a considerable increase in temperature, particularly in shock waves or regions of high shear. This can result in complex temperature profiles with sharp gradients. Effect on Heat Transfer Efficiency: A higher Eckert number generally reduces the efficiency of heat transfer processes. The additional heat generated by viscous dissipation must be accounted for in the energy balance, leading to a modified temperature distribution. This effect is particularly important in systems where precise temperature control is critical, such as in aerospace engineering or high-speed flow systems. Flow Regime Dependence: The influence of the Eckert number on temperature distribution depends on the flow regime. In laminar flows, the effect of viscous dissipation is more localized, leading to a more predictable increase in temperature near solid boundaries. In turbulent flows, the effect can be more widespread due to the mixing and redistribution of heat throughout the flow. The deviations of temperature distributions with impact of Prandtl number (Pr) are displayed in Fig. 9. The Prandtl number plays crucial role in determining relative thicknesses of velocity and thermal boundary layers in fluid flows. The effect of Prandtl number on temperature profiles can be understood through following points: The Prandtl number indicates relationship between velocity and thermal boundary layers, which represents relative thickness of velocity boundary layer (where momentum is diffused) and thermal boundary layer (where heat is diffused). A higher Prandtl number implies that momentum diffuses more rapidly than heat, leading to a thinner thermal boundary layer than velocity boundary layer. Conversely, a lower Prandtl number indicates that heat

diffuses more quickly, resulting in thicker thermal boundary layer. High Prandtl Number (Pr¿1): In fluids with high Prandtl numbers (such as oils), thermal diffusivity is low compared to momentum diffusivity. This leads to a thin thermal boundary layer. As a result, temperature gradient near wall is steep, meaning that temperature changes occur more rapidly over a smaller distance from the wall. The velocity boundary layer, being thicker, influences overall flow, but temperature profile is dominated by sharp gradients within the thin thermal layer. Low Prandtl Number (Pr¡ 1): In fluids with low Prandtl numbers (such as liquid metals), thermal diffusivity is high relative to momentum diffusivity. This results in a thicker thermal boundary layer compared to velocity boundary layer. The temperature gradient near wall is more gradual, leading to a smoother temperature profile. The thicker thermal boundary layer allows for more extended regions of heat transfer, spreading temperature distribution over a larger distance. Prandtl Number Equal to 1 (Pr 1): When Prandtl number is around 1 (e.g., in air), the thicknesses of velocity and thermal boundary layers are comparable. In such cases, temperature and velocity profiles develop simultaneously, leading to a balanced and consistent distribution of temperature and velocity gradients across boundary layers. Impact on Heat Transfer Rate: The Prandtl number directly influences heat transfer rate in a fluid. For high Prandtl number fluids, steep temperature gradients in thin thermal boundary layer result in higher local heat transfer rates near wall. In contrast, with their gradual temperature gradients, low Prandtl number fluids tend to have a lower local heat transfer rate but over a broader region. Convection-Dominated vs. Conduction-Dominated Heat Transfer: In convection-dominated systems (high Prandtl number), fluid flow significantly affects temperature profile, with heat being carried away from boundary by convection. In conduction-dominated systems (low Prandtl number), temperature profile is more influenced by heat conduction, leading to a smoother and more uniform distribution. Fig. 10 can be inferred the changes in temperature profile with influence of radiation parameter. The $\theta(\eta)$ enhances when we accelerate because the radiation parameter plays an important role in heat transfer when thermal radiation significantly affects energy exchange within a system. It quantifies impact of radiative heat transfer compared to other modes, such as conduction and convection. The radiation parameter plays a crucial role in influencing temperature profile in systems where radiative heat exchange is significant—this includes high-temperature processes, porous media, and applications involving radiative cooling or heating. When radiation parameter is low, conduction becomes predominant mode of heat transfer, rendering radiative effects negligible. In such scenarios, temperature distribution adheres to the classical pattern of conductive heat transfer. For straightforward cases, like steady-state conduction through a slab with constant thermal conductivity, the temperature profile typically exhibits a linear progression. In this context, conductive heat flow primarily influences temperature variations, while radiative heat transfer minimizes the overall temperature gradient. The deviations of $\phi(\eta)$ is indicated in Fig. 11. When we rise Sc values concentration decelerates. The Schmidt number affects thickness of concentration boundary layer in systems involving mass transfer, such as in chemical reactors or air-water interfaces. For high Sc, boundary layer is thin, meaning that

diffusion occurs over a small distance from surface, which causes concentration gradient to be steep near interfaces. For low Sc, the boundary layer is thicker, and solute spreads over larger distance, resulting in a more gradual concentration change. The consequences of Brownian motion (Nb) on $\phi(\eta)$ is displayed in Fig.12. Brownian motion leads to a decrease in concentration gradients and promotes an even distribution of particles by diffusing them from areas of high concentration to low concentration. Because Brownian motion is closely linked to the process of diffusion, where particles move from areas of high concentration to areas of low concentration. Due to random collisions, particles spread out over time, leading to a more uniform concentration. Nb helps in mixing of substances at the microscopic level, leading to a more uniform concentration. Without it, particles would take longer to mix, especially in liquids or gases. Initially, in areas of high concentration, Nb causes particles to move away, reducing concentration locally. Over time, this leads to an even distribution across system. If there is no external force (like gravity or convection), Brownian motion will eventually lead to equilibrium, where concentration of particles is same throughout the system. Nb is more noticeable in smaller particles. Larger particles move more slowly due to their higher mass, which reduces effect of Nb on their concentration over time.

References

1. S. U. S. Choi, Enhancing Thermal Conductivity of Fluids with Nanoparticles, *The Proceedings of the 1995 ASME Int. Mechanical Engineering Congress and Exposition,* ASME, San Francisco, USA, FED 231/MD, (1995), Vol. **66**, p. 99.
2. M.Sbragaglia and A.Prosperetti, Effective velocity boundary condition at a mixed slip surface.*Journal of Fluid Mechanics*,Volume **578**, 10 May 2007, pp. 435–451. DOI: https://doi.org/10.1017/S0022112007005149https://doi.org/10.1017/S0022112007005149.
3. W. K. Khan and I. Pop, *Int. J. of Heat and Mass Transfer* **53**, 2477 (2010).
4. Aly, E. H., Effect of the Velocity Slip Boundary Condition on the Flow and Heat Transfer of Nanofluids Over a Stretching Sheet. *J*ournal of Computational and Theoretical Nanoscience, **12**(9), 2428–2436. :10.1166/jctn.2015.4043.
5. M. R. Krishnamurthy, B. C. Prasannakumara, B. J. Gireesha, and R. S. R. Gorla, Effect of chemical reaction on MHD boundary layer flow and melting heat transfer of Williamson nanofluid in porous medium.*E*ng. Sci. Tech. an Int. J. **19**, 53 (2016).
6. A. M. Siddiqui, S. Bhatti, M. A. Rana, and M. Zahid, *B*lade coating analysis of a Williamson fluid Results in Physics **7**, 2845 (2017).
7. M. V. Krishna and A. J. Chamkha, Heat and mass transfer on MHD flow of Second grade fluid through porous medium over a semi-infinite vertical stretching sheet. *J*ournal of Porous Media **22**, 209 (2019).
8. Kebede T., Haile E., Awgichew G., Walelign T. Heat and Mass Transfer in Unsteady Boundary Layer Flow of Williamson Nanofluids.*J*ournal of Applied Mathematics, 2020, 1–13. DOI:doi:10.1155/2020/1890972
9. Mansur S. Ishak A. The Magnetohydrodynamic Boundary Layer Flow of a Nanofluid past a Stretching/Shrinking Sheet with Slip Boundary Conditions. *J*ournal of Applied Mathematics, 2014, 1–7. DOI:doi:10.1155/2014/907152.
10. A. J. Chamkha, A. S. Dogonchi, and D. D. Ganji, Magnetohydrodynamic Nanofluid Natural Convection in a Cavity under Thermal Radiation and Shape Factor of Nanoparticles Impacts: A Numerical Study Using CVFEM. *A*pplied Sciences **8**, 2396 (2018).
11. A. S. Dogonchi, S. M. Seyyedi, M. Hashemi-Tilehnoee, A. J. Chamkha, and D. D. Ganji, Investigation of natural convection of magnetic nanofluid in an enclosure with a porous medium considering Brownian motion.*C*ase Studies in Thermal Engineering **14**, 100502 (2019). https://doi.org/10.1016/j.csite.2019.100502.

12. Sejunti M. and Khaleque T. Effects of Velocity and Thermal Slip Conditions with Radiation on Heat Transfer Flow of Ferrofluids. *J*ournal of Applied Mathematics and Physics, **7**, 1369-1387.DOI: 10.4236/jamp.2019.76092.
13. M. V. Krishna and A. J. Chamkha, Hall and ion slip effects on Unsteady MHD Convective Rotating flow of Nanofluids-Application in Biomedical Engineering. *J*ournal of the Egyptian Mathematical Society **28**, 1 (2020).
14. Ruifei Wang, Jin Chai, Bobo Luo, Xiong Liu, Jianting Zhang, Min Wu, Mingdan Wei1 and Zhuanyue Ma, A review on slip boundary conditions at the nanoscale: recent development and applications. *B*eilstein J. Nanotechnol. 2021, **12**, 1237–1251. https://doi.org/10.3762/bjnano.12.91.
15. Hussan Zeb, Hafiz Abdul Wahab, Umar Khan, Amnah S.Al Juhani, Mulugeta Andualem, Ilyas Khan, The Velocity Slip Boundary Condition Effects on Non-Newtonian Ferrofluid over a Stretching Sheet.*M*athematical Problems in Engineering. 17 May 2022, https://doi.org/10.1155/2022/1243333.
16. Mohamed Kezzar, Nabil Talbi, Mohamed Rafik Sari, Abdelaziz Nehal, Mohsen Sharifpur , Ravinder Kumar, Nima Gharib, Wafa Salsoul, Haddad Fatiha, Velocity-slip boundary conditions and shape factor effects on MHD hybrid nanofluid flow via converging/diverging channels. *J*ournal of Magnetism and Magnetic Materials, Volume **587**, 1 December 2023, 171215. https://doi.org/10.1016/j.jmmm.2023.171215.
17. A.S. Dawood, Faisal A. Kroush, Ramzy M. Abumandour and Islam M. Eldesoky, Effect of slip boundary conditions on unsteady pulsatile nanofluid flow through a sinusoidal channel: an analytical study. *S*pringer Open Journal, (2024) 2024:59 https://doi.org/10.1186/s13661-024-01862-2.
18. Hui WU, Weifang CHEN, Zhongzheng JIANG, Slip boundary conditions for rough surfaces. *C*hinese Journal of Aeronautics, Volume **36**, Issue 5, May 2023, Pages 239-249. https://doi.org/10.1016/j.cja.2023.02.002.
19. Azad Hussain, Nevzat Akkurt, Aysha Rehman, Haifaa F. Alrihieli, Fahad M. Alharbi, Aishah Abdussattar Sayed M. Eldin, Transportation of thermal and velocity slip factors on three-dimensional dual phase nanomaterials liquid flow towards an exponentially stretchable surface. *Scientific Reports.* 2022 Nov 3;**12**(1):18595https://doi.org/10.1038/s41598-022-21966-y
20. Al- Zubaidi, Hajar Abutuqayqah, Bilal Ahmad, Sadaf Bibi, Tasawar Abbas, S. Saleem, Analysis of slip condition in MHD nanofluid flow over stretching sheet in presence of viscous dissipation: Keller box simulations. *A*lexandria Engineering Journal, Volume **82**, 1 November 2023, Pages 26-34.
21. Lavanya B, Pai RG, Raveendra N, Kemparaju M C, Multiple Slip Effects on the Time Independent MHD Flow of a UCM Fluid over an Elongating Surface That Has Higher-Grade Chemical Reaction. *I*nternational Journal of Heat Technology 2024 Feb 1;**42**(1).
22. Saquib Ul Zaman, Muhammad Nauman Aslam, Muhammad Bilal Riaz, Ali Akgul, Azad Hussan, Williamson MHD nanofluid flow with radiation effects through slender cylinder. *R*esults in Engineering, Volume **22**, June 2024, 101966.
23. M. Siva Sankari, M. Eswara Rao, Zill E. Shams, Salem Algarni, Muhammad Nadeem Sharif, Talal Alqahtani, Mohamed R. Eid, Wasim Jamshed, Kashif Irshad, Williamson MHD nanofluid flow via a porous exponentially stretching sheet with bioconvective fluxes.*C*ase Studies in Thermal Engineering, Volume **59**, July 2024, 104453.
24. M Vinodkumar Reddy, M Ajithkumar,and Anwar Saeed, Magneto-Williamson nanofluid flow past a wedge with activation energy: Buongiorno model.*Advances in Mechanical Engineering.* 2024 Jan;**16**(1):1687813223122302

Department of Mathematics, CIIRC, Jyothy Institute of Technology, Bengaluru, Visvesvaraya Technological University, Belagavi, Karnataka, India.
Email address: kemparajumc@gmail.com

Department of Mathematics, Manipal Institute of Technology, Manipal Academy of Higher Education, Manipal, Karnataka 576104, India.
Email address: lavanya.b@manipal.edu.

Department of Mathematics, Rajarajeswari College of Engineering, Bengaluru, Visvesvaraya Technological University, Belagavi, Karnataka, India.
Email address: r.ravi1505@gmai

Department of Studies and Research in Mathematics, Government College (Autonomous), Kalaburagi, Karnataka, India.
Email address: nandeppanavarmm@gmail.com

Department of Mathematics, KS School of Engineering and Management, Bengaluru, Visvesvaraya Technological University, Belagavi, Karnataka, India.
Email address: nagu17.12@gmail.com